

Supporting Information

Syntheses, Structures, and Magnetic Properties of Lanthanide Complexes of Imidazole-Substituted Nitronyl Nitroxide Biradicals

Cheng-Cai Xia,^a Wen-Jie Ji,^a Xin-Yu Zhang,^a Hao Miao,^a Yi-Quan Zhang^{*b} and Xin-Yi Wang^{*a}

^aState Key Laboratory of Coordination Chemistry, Collaborative Innovation Center of Advanced Microstructures, School of Chemistry and Chemical Engineering, Nanjing University, Nanjing, 210023, China. E-mail: wangxy66@nju.edu.cn

^bJiangsu Key Laboratory for NSLSCS, School of Physical Science and Technology, Nanjing Normal University, Nanjing 210023, China. E-mail: zhangyiquan@nju.edu.cn

1.	X-ray crystallography and powder x-ray diffraction	2
	Table S1 Selected bond lengths [Å] and angles [°] for complex 1 _{Gd}	2
	Table S2 Selected bond lengths [Å] and angles [°] for complex 2 _{Tb}	3
	Table S3 Selected bond lengths [Å] and angles [°] for complex 3 _{Dy}	4
	Table S4 Selected bond lengths [Å] and angles [°] for complex 4 _{Gd}	4
	Table S5 Selected bond lengths [Å] and angles [°] for complex 5 _{Tb}	5
	Table S6 Selected bond lengths [Å] and angles [°] for complex 6 _{Dy}	5
	Table S7 SHAPE analyses for 1 _{Gd} –6 _{Dy}	6
	Figure S1 X-ray powder diffraction patterns of complexes 1 _{Gd} –6 _{Dy}	7
2.	Synthesis of BNITImH-C2/-C4 biradicals and Packing diagrams of 1 _{Gd} –6 _{Dy}	7
	Scheme S1 The synthesis of BNITImH-C2/-C4 biradicals.	7
	Figure S2 The chiral helical chains of 1 _{Gd} –3 _{Dy} along b axis in which H, F, MeOH molecules and nitrates are omitted for clarity. The helical chains are all of the same right-hand helix....	8
	Figure S3 Packing diagram of 1 _{Gd} –3 _{Dy} (H, F, and MeOH molecules are omitted).	8
	Figure S4 Packing diagram of 4 _{Gd} –6 _{Dy} (H, F, and toluene molecules are omitted).....	8
3.	Magnetic Properties	9
	Figure S5 Frequency-dependent ac signals for 2 _{Tb} (left) and 3 _{Dy} (right) at 2 K under a 1000 Oe dc field.	9
	Figure S6 Frequency-dependent ac signals for 6 _{Dy} at 2 K under a 0 Oe dc field.	9
	Table S8 Relaxation fitting parameters from the least-square fitting of the Cole-Cole plots of 5 _{Tb} under a 0 Oe dc field according to the generalized Debye model.....	9
	Table S9 Relaxation fitting parameters from the least-square fitting of the Cole-Cole plots of 5 _{Tb} under a 1000 Oe dc field according to the generalized Debye model.....	10
4.	Details for calculations	10
	Figure S7 Calculated structures of complexes 2 _{Tb} and 5 _{Tb} ; H atoms are omitted for clarity...11	11
	Figure S8 Calculated orientations of the local main magnetic axes in the ground spin-orbit states on Tb ^{III} ions of 2 _{Tb} and 5 _{Tb}	11

Table S10 Calculated energy levels (cm^{-1}), g (g_x, g_y, g_z) tensors, and predominant m_J values of the lowest seven spin-orbit states of individual Tb^{III} fragments of complexes 2_{Tb} and 5_{Tb} using CASSCF/RASSI-SO with OpenMolcas.....	11
Table S11 Wave functions with definite projections of the total moment $ m_J \rangle$ for the lowest two spin-orbit states of individual Tb^{III} fragments of 2_{Tb} and 5_{Tb} using CASSCF/RASSI-SO with OpenMolcas.....	12
Table S12 Calculated crystal-field parameters $B(k, q)$ and the corresponding weights for individual Tb^{III} fragments of 2_{Tb} and 5_{Tb} using CASSCF/RASSI-SO with OpenMolcas.....	12
Table S13 Exchange energies E (cm^{-1}) and the main values of the g_z for the lowest two or four exchange doublets of 2_{Tb} and 5_{Tb}	13
Figure S9 Calculated (red solid line) and experimental (black circle dot) data of magnetic susceptibilities of 2_{Tb} and 5_{Tb} . The intermolecular interaction parameters zJ' of 2_{Tb} and 5_{Tb} were fitted to 0.000 and 0.020 cm^{-1} , respectively	14

1. X-ray crystallography and powder x-ray diffraction

Table S1 Selected bond lengths [\AA] and angles [$^\circ$] for complex **1_{Gd}**.

Gd(1)-O(2)	2.399(2)	O(7)-Gd(1)-O(11)	131.88(9)
Gd(1)-O(4) ^{#1}	2.416(2)	O(7)-Gd(1)-O(13)	155.32(9)
Gd(1)-O(5)	2.603(3)	O(7)-Gd(1)-N(3)	115.20(9)
Gd(1)-O(7)	2.470(3)	O(7)-Gd(1)-N(6) ^{#1}	71.67(9)
Gd(1)-O(8)	2.463(3)	O(8)-Gd(1)-O(5)	70.06(9)
Gd(1)-O(10)	2.480(3)	O(8)-Gd(1)-O(7)	78.15(9)
Gd(1)-O(11)	2.539(3)	O(8)-Gd(1)-O(10)	52.09(10)
Gd(1)-O(13)	2.498(3)	O(8)-Gd(1)-O(11)	116.86(10)
Gd(1)-N(3)	2.601(3)	O(8)-Gd(1)-O(13)	124.94(10)
Gd(1)-N(6) ^{#1}	2.604(3)	O(8)-Gd(1)N(3)	76.70(8)
O(1)-N(1)	1.266(4)	O(8)-Gd(1)N(6) ^{#1}	74.21(9)
O(2)-N(2)	1.285(3)	O(10)-Gd(1)-O(5)	115.66(9)
O(3)-N(8)	1.278(4)	O(10)-Gd(1)-O(11)	69.68(10)
O(4)-N(7)	1.291(3)	O(10)-Gd(1)-O(13)	78.31(10)
O(2)-Gd(1)-O(4) ^{#1}	70.73(8)	O(10)-Gd(1)N(3)	75.34(8)
O(2)-Gd(1)-O(5)	70.33(9)	O(10)-Gd(1)N(6) ^{#1}	76.13(9)
O(2)-Gd(1)-O(7)	88.24(9)	O(11)-Gd(1)-O(5)	172.70(10)
O(2)-Gd(1)-O(8)	137.35(9)	O(11)-Gd(1)-N(3)	112.78(9)
O(2)-Gd(1)-O(10)	140.89(9)	O(11)-Gd(1)-N(6) ^{#1}	69.93(9)
O(2)-Gd(1)-O(11)	102.37(9)	O(13)-Gd(1)-O(5)	124.71(8)
O(2)-Gd(1)-O(13)	68.89(9)	O(13)-Gd(1)-O(11)	50.07(9)
O(2)-Gd(1)-N(3)	73.05(8)	O(13)-Gd(1)-N(3)	68.03(9)
O(2)-Gd(1)-N(6) ^{#1}	138.94(8)	O(13)-Gd(1)-N(6) ^{#1}	119.71(9)
O(4) ^{#1} -Gd(1)-O(5)	105.18(8)	N(3)-Gd(1)-O(5)	65.47(9)
O(4) ^{#1} -Gd(1)-O(7)	67.89(9)	N(3)-Gd(1)-N(6) ^{#1}	147.85(8)
O(4) ^{#1} -Gd(1)-O(8)	135.58(9)	N(2)-O(2)-Gd(1)	131.03(18)

O(4) ^{#1} -Gd(1)-O(10)	134.52(9)	N(7)-O(4)-Gd(1) ^{#2}	124.61(19)
O(4) ^{#1} -Gd(1)-O(11)	71.80(9)	O(4) ^{#1} -Gd(1)-N(3)	143.55(8)
O(4) ^{#1} -Gd(1)-O(13)	94.85(9)	O(4) ^{#1} -Gd(1)-N(6) ^{#1}	68.59(8)
O(5)-Gd(1)-N(6) ^{#1}	115.57(9)	O(7)-Gd(1)-O(10)	126.35(9)
O(7)-Gd(1)-O(5)	49.88(8)		

Symmetry transformations used to generate equivalent atoms: ^{#1} 1-X,1/2+Y,1/2-Z; ^{#2} 1-X,-1/2+Y,1/2-Z

Z

Table S2 Selected bond lengths [Å] and angles [°] for complex **2_{Tb}**.

Tb(1)-O(8)	2.606(4)	O(4) ^{#1} -Tb(1)-O(7)	136.93(14)
Tb(1)-O(2)	2.399(4)	N(6) ^{#1} -Tb(1)-O(8)	65.39(14)
Tb(1)-O(4) ^{#1}	2.387(3)	O(13)-Tb(1)-O(8)	124.40(13)
Tb(1)-N(6) ^{#1}	2.591(5)	O(13)-Tb(1)-N(6) ^{#1}	67.86(14)
Tb(1)-O(13)	2.479(4)	O(13)-Tb(1)-O(11)	50.58(14)
Tb(1)-O(11)	2.535(4)	O(13)-Tb(1)-N(3)	120.04(14)
Tb(1)-O(10)	2.447(4)	O(11)-Tb(1)-O(8)	173.00(16)
Tb(1)-N(3)	2.590(5)	O(11)-Tb(1)-N(6) ^{#1}	112.93(14)
Tb(1)-O(5)	2.468(4)	O(11)-Tb(1)-N(3)	69.75(15)
Tb(1)-O(7)	2.449(4)	O(10)-Tb(1)-O(8)	50.10(14)
O(2)-N(2)	1.297(6)	O(10)-Tb(1)-N(6) ^{#1}	115.32(14)
O(1)-N(1)	1.281(6)	O(10)-Tb(1)-O(13)	155.43(15)
N(9)-O(9)	1.221(6)	O(10)-Tb(1)-O(11)	131.66(14)
O(4)-N(7)	1.275(5)	O(10)-Tb(1)-N(3)	71.52(15)
O(3)-N(8)	1.274(6)	O(10)-Tb(1)-O(5)	125.98(15)
O(2)-Tb(1)-O(8)	105.44(14)	O(10)-Tb(1)-O(7)	78.02(15)
O(2)-Tb(1)-N(6) ^{#1}	143.63(13)	N(3)-Tb(1)-O(8)	115.56(14)
O(2)-Tb(1)-O(13)	94.77(14)	N(3)-Tb(1)-N(6) ^{#1}	147.44(15)
O(2)-Tb(1)-O(11)	71.67(14)	O(5)-Tb(1)-O(8)	115.63(15)
O(2)-Tb(1)-O(10)	68.13(15)	O(5)-Tb(1)-N(6) ^{#1}	75.45(14)
O(2)-Tb(1)-N(3)	68.92(14)	O(5)-Tb(1)-O(13)	78.58(15)
O(2)-Tb(1)-O(5)	134.27(14)	O(5)-Tb(1)-O(11)	69.49(16)
O(2)-Tb(1)-O(7)	135.82(14)	O(5)-Tb(1)-N(3)	75.67(15)
O(4) ^{#1} -Tb(1)-O(8)	69.96(13)	O(7)-Tb(1)-O(8)	69.92(14)
O(4) ^{#1} -Tb(1)-O(2)	70.73(13)	O(7)-Tb(1)-N(6) ^{#1}	76.47(14)
O(4) ^{#1} -Tb(1)-N(6) ^{#1}	73.19(13)	O(7)-Tb(1)-O(13)	124.89(15)
O(4) ^{#1} -Tb(1)-O(13)	69.12(14)	O(7)-Tb(1)-O(11)	116.70(16)
O(4) ^{#1} -Tb(1)-O(11)	103.05(15)	O(7)-Tb(1)-N(3)	74.06(16)
O(4) ^{#1} -Tb(1)-O(10)	88.08(15)	O(7)-Tb(1)-O(5)	52.05(15)
O(4) ^{#1} -Tb(1)-N(3)	139.17(14)	N(2)-O(2)-Tb(1)	124.8(3)
O(4) ^{#1} -Tb(1)-O(5)	141.39(14)	N(7)-O(4)-Tb(1) ^{#2}	131.6(3)

Symmetry transformations used to generate equivalent atoms: ^{#1} 1-X, -1/2+Y, 1/2-Z; ^{#2} 1-X, 1/2+Y, 1/2-Z

Table S3 Selected bond lengths [\AA] and angles [$^\circ$] for complex **3_{Dy}**.

Dy(1)-O(4) ^{#1}	2.407(3)	N(7)-O(4)-Dy(1) ^{#2}	123.8(2)
Dy(1)-O(2)	2.378(3)	N(2)-O(2)-Dy(1)	130.5(2)
Dy(1)-O(5)	2.633(3)	N(6) ^{#1} -Dy(1)-O(5)	116.40(11)
Dy(1)-O(7)	2.437(3)	N(3)-Dy(1)-O(5)	65.03(10)
Dy(1)-O(8)	2.438(3)	N(3)-Dy(1)-N(6) ^{#1}	147.95(11)
Dy(1)-O(10)	2.438(3)	O(7)-Dy(1)-O(5)	49.91(10)
Dy(1)-O(13)	2.487(3)	O(7)-Dy(1)-O(8)	77.08(11)
Dy(1)-O(11)	2.526(3)	O(7)-Dy(1)-O(10)	124.92(12)
Dy(1)-N(6) ^{#1}	2.546(3)	O(7)-Dy(1)-O(13)	156.00(12)
Dy(1)-N(3)	2.545(3)	O(7)-Dy(1)-O(11)	132.02(10)
O(4)-N(7)	1.293(4)	O(7)-Dy(1)-N(6) ^{#1}	71.38(11)
O(3)-N(8)	1.269(5)	O(7)-Dy(1)-N(3) ^{#1}	114.53(11)
O(1)-N(1)	1.280(5)	O(8)-Dy(1)-O(5)	70.21(11)
O(2)-N(2)	1.290(4)	O(8)-Dy(1)-O(13)	124.79(11)
O(4) ^{#1} -Dy(1)-O(5)	103.72(10)	O(8)-Dy(1)-O(11)	118.99(12)
O(4) ^{#1} -Dy(1)-O(7)	68.45(11)	O(8)-Dy(1)-N(6) ^{#1}	75.56(11)
O(4) ^{#1} -Dy(1)-O(8)	136.73(11)	O(8)-Dy(1)-N(3)	75.44(11)
O(4) ^{#1} -Dy(1)-O(10)	134.91(11)	O(10)-Dy(1)-O(5)	116.92(11)
O(4) ^{#1} -Dy(1)-O(13)	95.05(11)	O(10)-Dy(1)-O(8)	52.52(12)
O(4) ^{#1} -Dy(1)-O(11)	71.68(11)	O(10)-Dy(1)-O(13)	79.07(12)
O(4) ^{#1} -Dy(1)-N(6) ^{#1}	69.32(11)	O(10)-Dy(1)-O(11)	70.55(12)
O(4) ^{#1} -Dy(1)-N(3)	142.73(10)	O(10)-Dy(1)-N(6) ^{#1}	75.46(11)
O(2)-Dy(1)-O(4) ^{#1}	69.21(10)	O(10)-Dy(1)-N(3)	76.23(11)
O(2)-Dy(1)-O(5)	69.47(11)	O(13)-Dy(1)-O(5)	123.27(10)
O(2)-Dy(1)-O(7)	88.93(11)	O(13)-Dy(1)-O(11)	50.33(10)
O(2)-Dy(1)-O(8)	136.62(11)	O(13)-Dy(1)-N(6) ^{#1}	120.32(11)
O(2)-Dy(1)-O(10)	141.98(11)	O(13)-Dy(1)-N(3)	67.86(11)
O(2)-Dy(1)-O(13)	68.44(11)	O(11)-Dy(1)-O(5)	170.44(12)
O(2)-Dy(1)-O(11)	100.97(11)	O(11)-Dy(1)-N(6) ^{#1}	70.37(11)
O(2)-Dy(1)-N(6) ^{#1}	138.22(10)	O(11)-Dy(1)-N(3)	113.30(11)
O(2)-Dy(1)-N(3)	73.65(10)		

Symmetry transformations used to generate equivalent atoms: ^{#1} 1-X, -1/2+Y, 3/2-Z; ^{#2} 1-X, 1/2+Y, 3/2-Z**Table S4** Selected bond lengths [\AA] and angles [$^\circ$] for complex **4_{Gd}**.

Gd(1)-O(2)	2.366(2)	O(2)-Gd(1)-O(3)	76.51(8)
Gd(1)-O(3)	2.388(2)	O(2)-Gd(1)-O(5)	141.49(7)
Gd(1)-O(4)	2.345(2)	O(2)-Gd(1)-O(6)	81.31(7)
Gd(1)-O(5)	2.370(2)	O(2)-Gd(1)-O(7)	142.12(7)
Gd(1)-O(6)	2.411(2)	O(2)-Gd(1)-N(2)	70.50(8)
Gd(1)-O(7)	2.372(2)	O(3)-Gd(1)-O(6)	147.29(8)
Gd(1)-O(8)	2.326(2)	O(3)-Gd(1)-N(2)	119.29(9)

Gd(1)-N(2)	2.520(2)	O(4)-Gd(1)-O(2)	108.56(8)
O(1)-N(3)	1.268(3)	O(4)-Gd(1)-O(3)	71.23(9)
O(2)-N(4)	1.296(3)	O(4)-Gd(1)-O(5)	78.01(8)
O(7)-Gd(1)-O(6)	112.56(8)	O(4)-Gd(1)-O(6)	139.67(8)
O(7)-Gd(1)-N(2)	146.10(8)	O(4)-Gd(1)-O(7)	83.96(8)
O(8)-Gd(1)-O(2)	77.29(8)	O(4)-Gd(1)-N(2)	73.13(8)
O(8)-Gd(1)-O(3)	76.07(8)	O(5)-Gd(1)-O(3)	138.27(8)
O(8)-Gd(1)-O(4)	144.00(8)	O(5)-Gd(1)-O(6)	71.81(7)
O(8)-Gd(1)-O(5)	120.16(8)	O(5)-Gd(1)-O(7)	75.22(7)
O(8)-Gd(1)-O(6)	75.80(7)	O(5)-Gd(1)-N(2)	75.80(8)
O(8)-Gd(1)-O(7)	72.84(8)	O(6)-Gd(1)-N(2)	73.98(8)
O(8)-Gd(1)-N(2)	138.42(8)	O(7)-Gd(1)-O(3)	74.13(8)
N(4)-O(2)-Gd(1)	126.89(17)		

Table S5 Selected bond lengths [Å] and angles [°] for complex **5_{Tb}**.

Tb(1)-O(2)	2.360(3)	O(2)-Tb(1)-O(3)	76.04(11)
Tb(1)-O(6)	2.395(3)	O(2)-Tb(1)-N(2)	70.76(11)
Tb(1)-O(5)	2.357(3)	O(6)-Tb(1)-N(2)	74.28(12)
Tb(1)-O(8)	2.317(3)	O(5)-Tb(1)-O(2)	141.78(10)
Tb(1)-O(7)	2.356(3)	O(5)-Tb(1)-O(6)	72.00(11)
Tb(1)-O(4)	2.332(3)	O(5)-Tb(1)-O(3)	138.56(11)
Tb(1)-O(3)	2.377(3)	O(5)-Tb(1)-N(2)	75.93(11)
Tb(1)-N(2)	2.505(4)	O(8)-Tb(1)-O(2)	76.98(11)
O(2)-N(4)	1.297(5)	O(8)-Tb(1)-O(6)	75.57(11)
O(1)-N(3)	1.263(5)	O(8)-Tb(1)-O(5)	120.14(12)
O(4)-Tb(1)-O(2)	108.85(12)	O(8)-Tb(1)-O(7)	73.41(11)
O(4)-Tb(1)-O(6)	139.82(11)	O(8)-Tb(1)-O(4)	144.06(11)
O(4)-Tb(1)-O(5)	77.88(12)	O(8)-Tb(1)-O(3)	75.92(12)
O(4)-Tb(1)-O(7)	83.32(12)	O(8)-Tb(1)-N(2)	138.45(11)
O(4)-Tb(1)-O(3)	71.56(12)	O(7)-Tb(1)-O(2)	142.13(10)
O(4)-Tb(1)-N(2)	73.05(12)	O(7)-Tb(1)-O(6)	112.89(11)
O(3)-Tb(1)-O(6)	146.79(11)	O(7)-Tb(1)-O(5)	74.98(11)
O(3)-Tb(1)-N(2)	119.09(13)	O(7)-Tb(1)-O(3)	74.28(12)
N(4)-O(2)-Tb(1)	126.8(2)	O(7)-Tb(1)-N(2)	145.65(11)
O(2)-Tb(1)-O(6)	81.27(11)		

Table S6 Selected bond lengths [Å] and angles [°] for complex **6_{Dy}**.

Dy(1)-O(2)	2.345(3)	O(2)-Dy(1)-O(3)	75.29(9)
Dy(1)-O(3)	2.364(3)	O(2)-Dy(1)-O(5)	142.31(9)
Dy(1)-O(4)	2.315(3)	O(2)-Dy(1)-O(6)	81.54(9)
Dy(1)-O(5)	2.349(3)	O(2)-Dy(1)-N(2)	70.87(9)
Dy(1)-O(6)	2.382(3)	O(3)-Dy(1)-O(6)	146.12(9)
Dy(1)-O(7)	2.343(3)	O(3)-Dy(1)-N(2)	119.11(11)
Dy(1)-O(8)	2.302(3)	O(4)-Dy(1)-O(2)	108.61(10)

Dy(1)-N(2)	2.500(3)	O(4)-Dy(1)-O(3)	71.94(10)
O(1)-N(3)	1.270(4)	O(4)-Dy(1)-O(5)	77.89(10)
O(2)-N(4)	1.299(4)	O(4)-Dy(1)-O(6)	140.09(9)
O(8)-Dy(1)-O(2)	77.21(10)	O(4)-Dy(1)-O(7)	83.21(10)
O(8)-Dy(1)-O(3)	75.76(10)	O(4)-Dy(1)-N(2)	73.11(10)
O(8)-Dy(1)-O(6)	75.23(9)	O(5)-Dy(1)-O(3)	138.84(9)
O(8)-Dy(1)-O(7)	73.43(9)	O(5)-Dy(1)-O(6)	72.31(9)
O(8)-Dy(1)-O(4)	144.11(9)	O(5)-Dy(1)-N(2)	76.18(10)
O(8)-Dy(1)-O(5)	119.78(10)	O(6)-Dy(1)-N(2)	74.44(10)
O(8)-Dy(1)-N(2)	138.48(9)	O(7)-Dy(1)-O(2)	142.09(9)
N(4)-O(2)-Dy(1)	126.9(2)	O(7)-Dy(1)-O(3)	74.65(10)
O(7)-Dy(1)-O(6)	112.81(10)	O(7)-Dy(1)-O(5)	74.57(9)
O(7)-Dy(1)-N(2)	145.52(10)		

Table S7 SHAPE analyses for **1_{Gd}-6_{Dy}**.

Label \ Complexes	1 _{Gd}	2 _{Tb}	3 _{Dy}	Label \ Complexes	4 _{Gd}	5 _{Tb}	6 _{Dy}
OBPY-10	17.392	17.330	17.499	HBPY-8	16.411	16.558	16.601
PPR-10	11.089	11.141	11.157	CU-8	9.273	9.342	9.364
PAPR-10	12.294	12.217	12.156	SAPR-8	0.390	0.351	0.351
JBCCU-10	11.163	10.988	10.795	TDD-8	1.460	1.504	1.506
JBCSAPR-10	3.972	3.842	3.928	JGBF-8	15.978	15.966	16.006
JMBIC-10	8.063	8.009	8.095	JETBPY-8	27.810	27.929	28.164
JATDI-10	16.957	16.899	17.078	JBTPR-8	2.122	2.122	2.081
JSPC-10	2.353	2.324	2.158	BTPR-8	1.812	1.809	1.793
SDD-10	4.261	4.300	4.163	JSD-8	4.094	4.122	4.099
TD-10	3.263	3.272	3.173	TT-8	10.079	10.141	10.147
HD-10	9.059	8.948	8.828	ETBPY-8	23.771	23.865	24.089

Code	Label	Symmetry	Shape
1	HBPY-8	D6h	Hexagonal bipyramid
2	CU-8	Oh	Cube
3	SAPR-8	D4d	Square antiprism
4	TDD-8	D2d	Triangular dodecahedron
5	JGBF-8	D2d	Johnson gyrobifastigium (J26)
6	JETBPY-8	D3h	Johnson elongated triangular bipyramid (J14)
7	JBTPR-8	C2v	Biaugmented trigonal prism (J50)
8	BTPR-8	C2v	Biaugmented trigonal prism
9	JSD-8	D2d	Snub diphenoid (J84)
10	TT-8	Td	Triakis tetrahedron
11	ETBPY-8	D3h	Elongated trigonal bipyramid

Code	Label	Symmetry	Shape
1	OBPY-10	D8h	Octagonal bipyramid
2	PPR-10	D5h	Pentagonal prism
5	PAPR-10	D5d	Pentagonal antiprism
6	JBCCU-10	D4h	Bicapped cube (J15)
7	JBCSAPR-10	D4d	Bicapped square antiprism (J17)
8	JMBIC-10	C2v	Metabidiminished icosahedron (J62)
9	JATDI-10	C3v	Augmented tridiminished icosahedron (J64)
10	JSPC-10	C2v	Sphenocorona (J87)
11	SDD-10	D2	Staggered Dodecahedron (2:6:2)
12	TD-10	C2v	Tetradecahedron (2:6:2)
13	HD-10	D4h	Hexadecahedron (2:6:2) or (1:4:4:1)

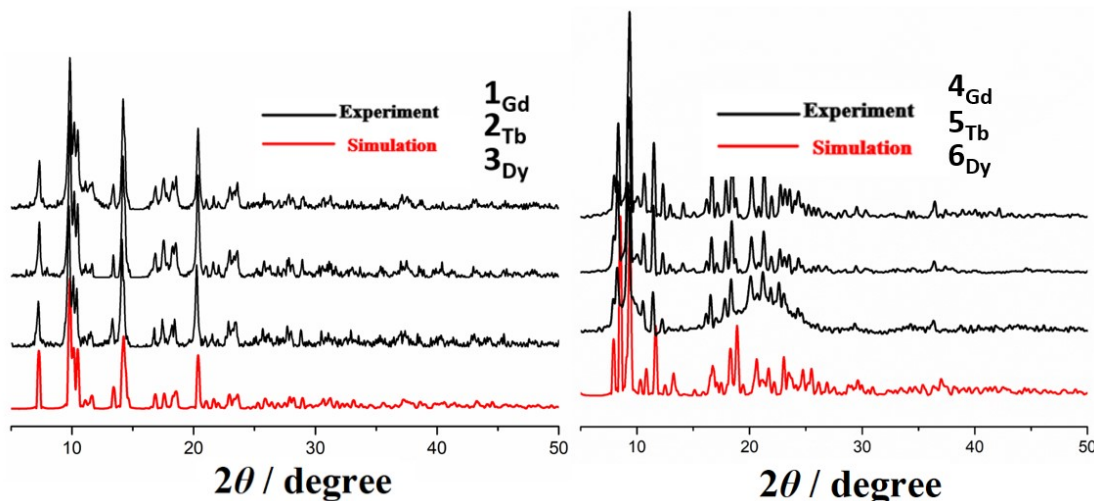
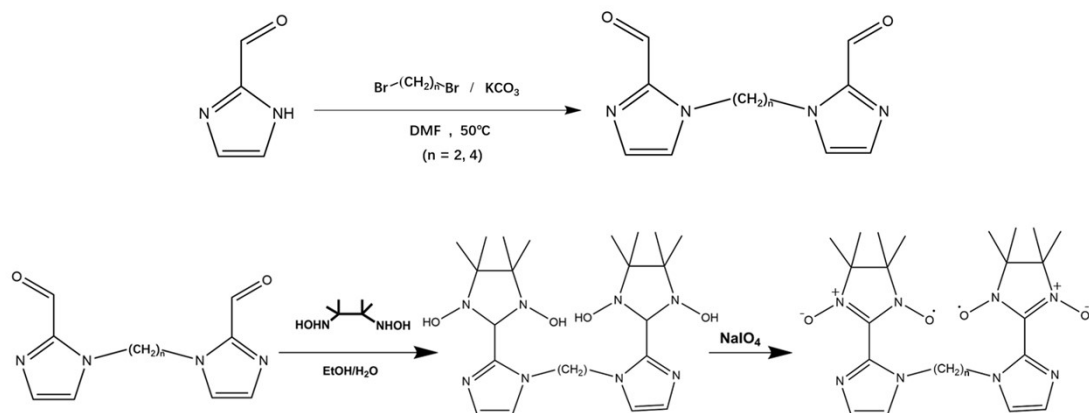


Figure S1 X-ray powder diffraction patterns of complexes $1_{\text{Gd}}\text{--}6_{\text{Dy}}$.

2. Synthesis of BNITImH-C2/-C4 biradicals and Packing diagrams of $1_{\text{Gd}}\text{--}6_{\text{Dy}}$



Scheme S1 The synthesis of BNITImH-C2/-C4 biradicals.

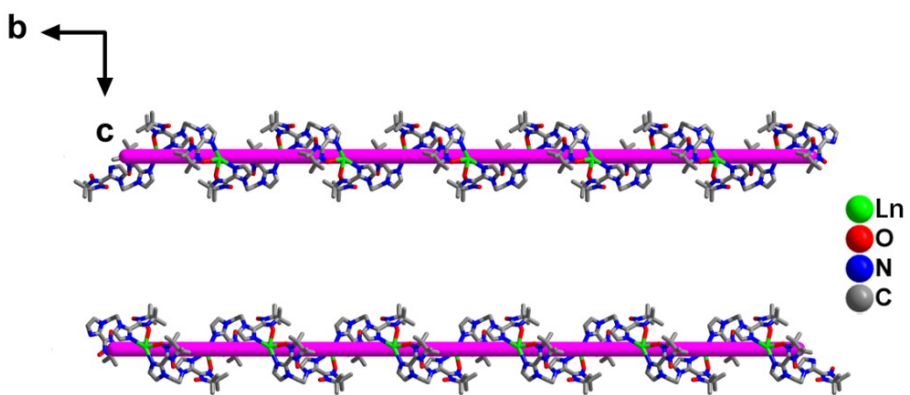


Figure S2 The chiral helical chains of $\mathbf{1}_{\text{Gd}}\text{--}\mathbf{3}_{\text{Dy}}$ along b axis in which H, F, MeOH molecules and nitrates are omitted for clarity. The helical chains are all of the same right-hand helix.

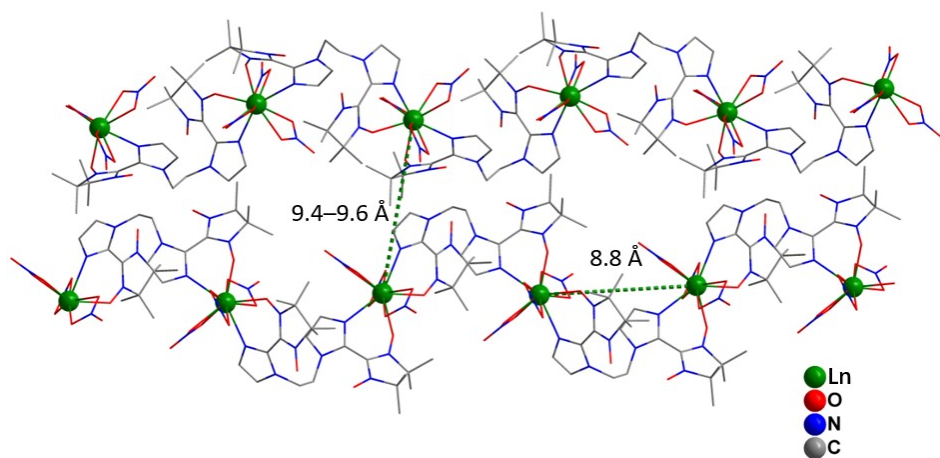


Figure S3 Packing diagram of $\mathbf{1}_{\text{Gd}}\text{--}\mathbf{3}_{\text{Dy}}$ (H, F, and MeOH molecules are omitted).

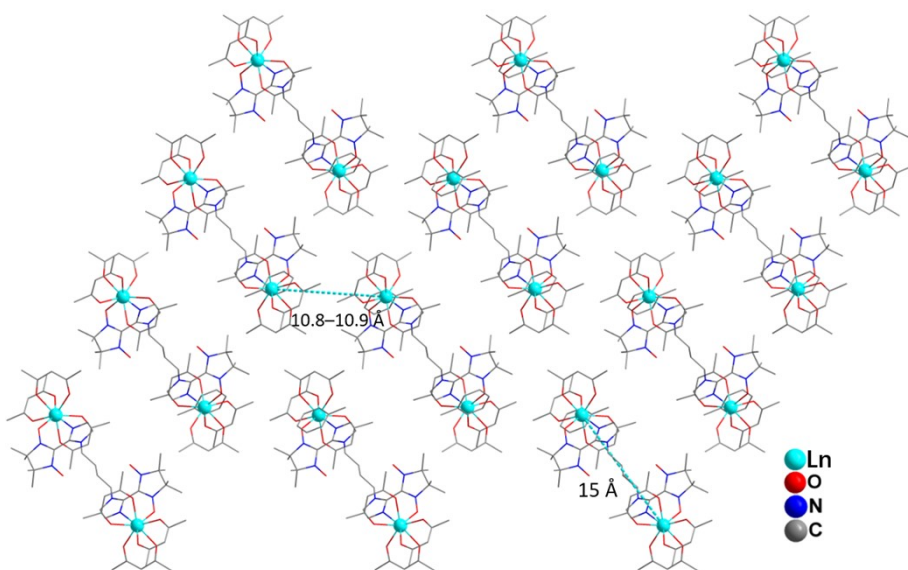


Figure S4 Packing diagram of $\mathbf{4}_{\text{Gd}}\text{--}\mathbf{6}_{\text{Dy}}$ (H, F, and toluene molecules are omitted).

3. Magnetic Properties

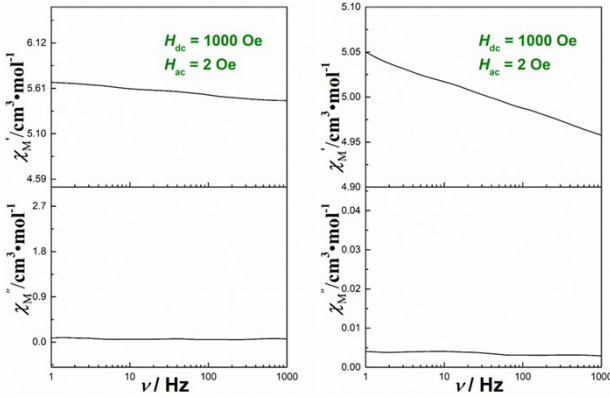


Figure S5 Frequency-dependent ac signals for **2Tb** (left) and **3Dy** (right) at 2 K under a 1000 Oe dc field.

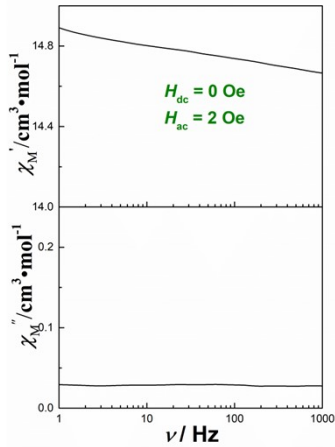


Figure S6 Frequency-dependent ac signals for **6Dy** at 2 K under a 0 Oe dc field.

Table S8 Relaxation fitting parameters from the least-square fitting of the Cole-Cole plots of **5Tb** under a 0 Oe dc field according to the generalized Debye model.

Temperature / K	$\chi_S / \text{cm}^3 \cdot \text{mol}^{-1} \cdot \text{K}$	$\chi_T / \text{cm}^3 \cdot \text{mol}^{-1} \cdot \text{K}$	τ / s	α
2.0	1.24	9.29	0.000428	0.31682
2.2	1.21	8.44	0.000411	0.29384
2.4	1.26	7.71	0.000390	0.25438
2.6	1.30	7.11	0.000348	0.20574
2.8	1.28	6.56	0.000280	0.15325
3.0	1.24	6.11	0.000212	0.11026
3.2	1.19	5.73	0.000153	0.081763
3.4	1.13	5.40	0.000108	0.064986
3.6	1.11	5.10	0.0000767	0.053987
3.8	0.955	4.84	0.0000519	0.053737
4.0	0.842	4.60	0.0000360	0.050788

Table S9 Relaxation fitting parameters from the least-square fitting of the Cole-Cole plots of **5_{Tb}** under a 1000 Oe dc field according to the generalized Debye model.

Temperature / K	$\chi_s / \text{cm}^3\text{mol}^{-1}\text{K}$	$\chi_T / \text{cm}^3\text{mol}^{-1}\text{K}$	τ / s	α
2.0	0.64	9.98	0.0570	0.45708
2.2	0.84	8.03	0.0174	0.28972
2.4	0.73	7.37	0.00719	0.23526
2.6	0.67	6.80	0.00289	0.17906
2.8	0.64	6.20	0.00126	0.13252
3.0	0.63	5.88	0.000617	0.11821
3.2	0.66	5.45	0.000325	0.093048
3.4	0.70	5.20	0.000190	0.087682
3.6	0.81	4.92	0.000120	0.068913
3.8	0.94	4.73	0.0000796	0.066294
4.0	0.11	4.51	0.0000558	0.055982
4.3	0.91	4.21	0.0000300	0.042262

4. Details for calculations

Complex **2_{Tb}** has two NO radicals while **5_{Tb}** has one NO radical. For each of them, the magnetic anisotropy energy barrier mainly comes from individual Tb^{III} ions considering the magnetic isotropy of NO radicals. Thus, complete-active-space self-consistent field (CASSCF) calculations on individual Tb^{III} fragments have been carried out with OpenMolcas^{S1} program package. During the above calculations, the spin values on all NO radicals have been set as zero by adding one electron to each of them. The calculated structures of complexes **2_{Tb}** and **5_{Tb}** are shown in Figure S7. The basis sets for all atoms are atomic natural orbitals from the ANO-RCC library: ANO-RCC-VTZP for Tb^{III}; VTZ for close O and N; VDZ for distant atoms. The calculations employed the second-order Douglas-Kroll-Hess Hamiltonian, where scalar relativistic contractions were considered in the basis set and the spin-orbit couplings were handled separately in the restricted active space state interaction (RASSI-SO) procedure.^{S2,S3} Active electrons in 7 active orbitals include all *f* electrons CAS(8 in 7) for Tb^{III} in the CASSCF calculations. To exclude all the doubts, we calculated all the roots in the active space. We have mixed the maximum number of spin-free states which was possible with our hardware (all from 7 septets, all from 140 quintets, and 68 from 500 triplets for Tb^{III}). SINGLE_ANISO^{S4–S6} program was used to obtain the energy levels, *g* tensors, magnetic axes, *et al.*, based on the above CASSCF/RASSI-SO calculations.

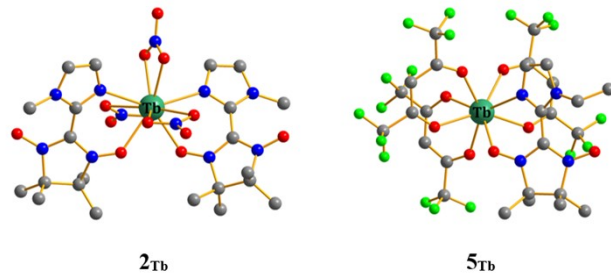


Figure S7 Calculated structures of complexes $\mathbf{2}_{\mathbf{Tb}}$ and $\mathbf{5}_{\mathbf{Tb}}$; H atoms are omitted for clarity.

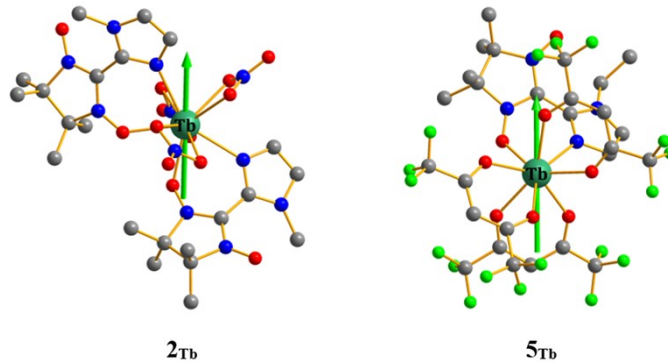


Figure S8 Calculated orientations of the local main magnetic axes in the ground spin-orbit states on Tb^{III} ions of $\mathbf{2}_{\mathbf{Tb}}$ and $\mathbf{5}_{\mathbf{Tb}}$.

Table S10 Calculated energy levels (cm^{-1}), \mathbf{g} (g_x, g_y, g_z) tensors, and predominant m_J values of the lowest seven spin-orbit states of individual Tb^{III} fragments of complexes $\mathbf{2}_{\mathbf{Tb}}$ and $\mathbf{5}_{\mathbf{Tb}}$ using CASSCF/RASSI-SO with OpenMolcas.

	$\mathbf{2} (\text{Tb}^{\text{III}})$			$\mathbf{5} (\text{Tb}^{\text{III}})$		
	E/cm^{-1}	\mathbf{g}	m_J	E/cm^{-1}	\mathbf{g}	m_J
1	0.0	0.000	± 6	0.0	0.000	± 6
	0.000				0.000	
	3.4	16.804		0.8	17.369	
2	26.1	0.000	± 5	81.0	0.000	± 5
	0.000				0.000	
	33.7	12.550		96.8	12.191	
3	45.9	0.000		116.0		
	54.3	0.000				
	80.2			129.5	0.000	
					0.000	
					15.374	

5	92.5	0.000		175.0	0.000	
	104.8	0.000 8.996		178.1	0.000 10.132	
6	108.6	0.000		264.2	0.000	
	111.6	0.000 14.740		264.4	0.000 13.580	
7	205.7	0.000		356.1	0.000	
	205.8	0.000 17.736		357.5	0.000 16.684	

Table S11 Wave functions with definite projections of the total moment $|m_J\rangle$ for the lowest two spin-orbit states of individual Tb^{III} fragments of **2_{Tb}** and **5_{Tb}** using CASSCF/RASSI-SO with OpenMolcas.

	E/cm^{-1}	wave functions
2_{Tb}	0.0	86.0% $ \pm 6\rangle + 6.2\% \pm 2\rangle$
	3.4	94.2% $ \pm 6\rangle$
	26.1	32.0% $ \pm 5\rangle + 31.2\% \pm 1\rangle + 21.4\% \pm 4\rangle + 9.6\% \pm 3\rangle$
	33.7	45.4% $ \pm 5\rangle + 23.8\% \pm 4\rangle + 16.4\% \pm 2\rangle + 4.9\% 0\rangle$
5_{Tb}	0.0	91.8% $ \pm 6\rangle$
	0.8	93.2% $ \pm 6\rangle$
	81.0	52.6% $ \pm 5\rangle + 27.4\% \pm 3\rangle + 15.8\% \pm 1\rangle$
	96.8	73.4% $ \pm 5\rangle + 19.8\% \pm 3\rangle$

Table S12 Calculated crystal-field parameters $B(k, q)$ and the corresponding weights for individual Tb^{III} fragments of **2_{Tb}** and **5_{Tb}** using CASSCF/RASSI-SO with OpenMolcas.

2 (Tb ^{III})				5 (Tb ^{III})			
k	q	$B(k, q)$	Weights (%)	k	q	$B(k, q)$	Weights (%)
2	-2	0.11×10^1	11.85	2	0	-0.17×10^1	12.24
2	1	0.91	9.77	2	1	0.17×10^1	11.92
2	0	-0.85	9.14	4	-4	0.13×10^{-1}	11.00
4	3	0.52×10^{-2}	6.57	4	1	-0.10×10^{-1}	8.23
2	-1	0.57	6.12	2	-2	-0.11×10^1	8.09
4	1	-0.46×10^{-2}	5.80	4	-2	-0.73×10^{-2}	6.03
2	2	0.48	5.18	4	2	0.73×10^{-2}	5.98
4	-1	-0.41×10^{-2}	5.12	4	0	-0.67×10^{-2}	5.50
6	6	-0.63×10^{-4}	4.58	2	2	0.71	5.01

To fit the exchange interactions between the magnetic centers and NO radicals in **2_{Tb}** and **5_{Tb}**, we took two steps to obtain them. Firstly, we calculated individual Tb^{III} fragments using

CASSCF/RASSI-SO to obtain the corresponding magnetic properties. Then, the exchange interactions between the magnetic centers and NO radicals were considered within the Lines model.^{S7} The Lines model is effective and has been successfully used in the research field of 3d and 4f-elements single-molecule magnets.^{S8,S9}

The Ising exchange Hamiltonian is:

$$\hat{H} = -2J_1(\hat{S}_{Rad1}\hat{S}_{Tb} + \hat{S}_{Rad2}\hat{S}_{Tb}) - 2J_2\hat{S}_{Rad1}\hat{S}_{Rad2} \quad \text{for } \mathbf{2}_{\text{Tb}} \quad (\text{S1}).$$

$$\hat{H} = -2J_1(\hat{S}_{Rad1}\hat{S}_{Tb1} + \hat{S}_{Rad2}\hat{S}_{Gd2}) \quad \text{for } \mathbf{5}_{\text{Tb}} \quad (\text{S2})$$

where J_1 is the parameter of the total effective magnetic coupling constant between Tb^{III} and NO with respect to the ground pseudospin of $\tilde{S}_{Tb} = 1/2$ on the Tb^{III} sites and the spin $S_{Rad} = 1/2$ on the NO radicals. J_2 is the parameter of the total magnetic coupling constant between NO radicals in $\mathbf{2}_{\text{Tb}}$. The Lines exchange coupling constants J ($\tilde{J}_1 = 6J_1$ and $\tilde{J}_2 = J_2$ for $\mathbf{2}_{\text{Tb}}$ and $\mathbf{5}_{\text{Tb}}$) were fitted through a comparison of the computed and measured magnetic susceptibilities using the POLY_ANISO program.^{S4-S6}

Table S13 Exchange energies E (cm⁻¹) and the main values of the g_z for the lowest two or four exchange doublets of $\mathbf{2}_{\text{Tb}}$ and $\mathbf{5}_{\text{Tb}}$.

	$\mathbf{2}_{\text{Tb}}$		$\mathbf{5}_{\text{Tb}}$	
	E/cm^{-1}	g_z	E/cm^{-1}	g_z
1	0.000	20.130	0.000	11.122
	0.055		0.000	
2	3.208	0.000	1.145	15.119
	3.891		1.145	
3	6.637	0.000		
	7.426			
4	11.367	11.641		
	11.540			

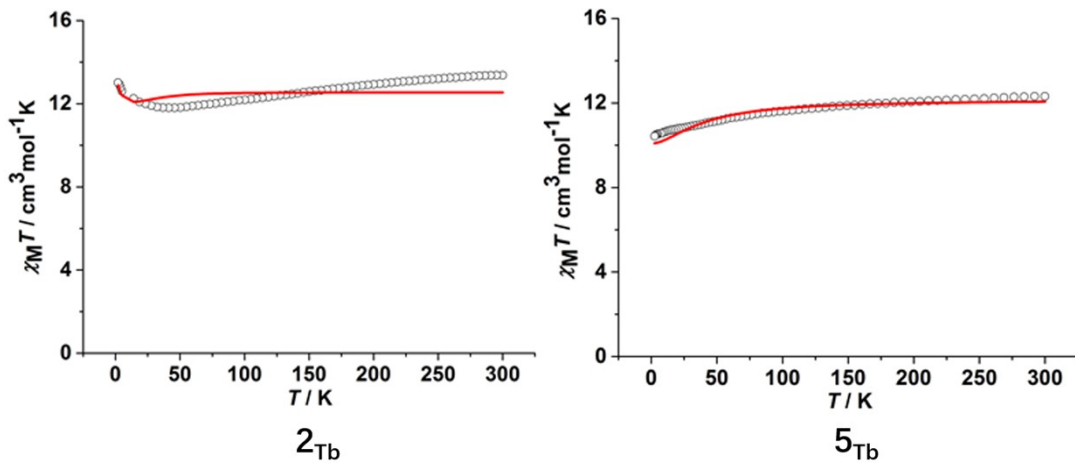


Figure S9 Calculated (red solid line) and experimental (black circle dot) data of magnetic susceptibilities of **2_{Tb}** and **5_{Tb}**. The intermolecular interaction parameters zJ' of **2_{Tb}** and **5_{Tb}** were fitted to 0.000 and 0.020 cm⁻¹, respectively.

References:

- S1 Galván, I. F.; Vacher, M.; Alavi, A.; Angeli, C.; Aquilante, F.; Autschbach, J.; Bao, J. J.; Bokarev, S. I.; Bogdanov, N. A.; Carlson, R. K.; Chibotaru, L. F.; Creutzberg, J.; Dattani, N.; Delcey, M. G.; Dong, S. S.; Dreuw, A.; Freitag, L.; Frutos, L. M.; Gagliardi, L.; Gendron, F.; Giussani, A.; González, L.; Grell, G.; Guo, M. Y.; Hoyer, C. E.; Johansson, M.; Keller, S.; Knecht, S.; Kovacevic, G.; Källman, E.; Manni, G. L.; Lundberg, M.; Ma, Y. J.; Mai, S.; Malhado, J. P.; Malmqvist, P. Å.; Marquetand, P.; Mewes, S. A.; Norell, J.; Olivucci, M.; Oppel, M.; Phung, Q. M.; Pierloot, K.; Plasser, F.; Reiher, M.; Sand, A. M.; Schapiro, I.; Sharma, P.; Stein, C. J.; Sørensen, L. K.; Truhlar, D. G.; Ugandi, M.; Ungur, L.; Valentini, A.; Vancoillie, S.; Veryazov, V.; Weser, O.; Wesołowski, T. A.; Widmark, Per-Olof.; Wouters, S.; Zech, A.; Zobel, J. P.; Lindh. *R. J. Chem. Theory Comput.* **2019**, *15*, 5925–5964.
- S2 Malmqvist, P. Å.; Roos, B. O.; Schimmelpfennig, B. *Chem. Phys. Lett.*, **2002**, *357*, 230–240.
- S3 Heß, B. A.; Marian, C. M.; Wahlgren, U.; Gropen, O. *Chem. Phys. Lett.*, **1996**, *251*, 365–371.
- S4 Chibotaru, L. F.; Ungur, L.; Soncini, A. *Angew. Chem., Int. Ed.* **2008**, *47*, 4126–4129.
- S5 Ungur, L.; Van den Heuvel, W.; Chibotaru, L. F. *New J. Chem.* **2009**, *33*, 1224–1230.
- S6 Chibotaru, L. F.; Ungur, L.; Aronica, C.; Elmoll, H.; Pilet, G.; Luneau, D. *J. Am. Chem. Soc.* **2008**, *130*, 12445–12455.
- S7 Lines, M. E. *J. Chem. Phys.* **1971**, *55*, 2977–2984.
- S8 Mondal, K. C.; Sundt, A.; Lan, Y. H.; Kostakis, G. E.; Waldmann, O.; Ungur, L.; Chibotaru, L. F.; Anson, C. E.; Powell, A. K. *Angew. Chem., Int. Ed.* **2012**, *51*, 7550–7554.
- S9 Langley, S. K.; Wielechowski, D. P.; Vieru, V.; Chilton, N. F.; Moubaraki, B.; Abrahams, B. F.; Chibotaru, L. F.; Murray, K. S. *Angew. Chem., Int. Ed.* **2013**, *52*, 12014–12019.